

# Forming simulation of textile composites using LS-DYNA

Masato Nishi, Tei Hirashima

JSOL Corporation

## 1 Abstract

The primary focus of this paper is on FE modeling and simulations performed, using LS-DYNA, to capture the material behaviors during textile reinforcement preform and thermoplastic resin pre-impregnated (pre-preg) sheet forming manufacturing. Although the out-of-plane bending stiffness of textile reinforcement is often ignored as it is very low compared to in-plane stiffness, more accurate simulation, especially the prediction of wrinkles, is achievable by considering out-of-plane bending stiffness in forming simulation. We propose a hybrid model which consists of a membrane and shells that can describe out-of-plane bending stiffness which is independent from in-plane behavior. In order to extend the textile reinforcement model to a thermoplastic pre-preg model for thermoforming simulation, temperature dependent stress contribution of thermoplastic is added to the textile reinforcement by applying Reuss model which can take the volume fraction of fiber ( $V_f$ ) into account.

## 2 Introduction

Carbon fiber reinforced plastic (CFRP) is a good alternative for metal used in load transmission structures. The increasing requirement for high performance with weight reduction in industry has gradually expanded the use of CFRP. One of the reasons for the expansion is that the development of resin transfer molding (RTM) has reduced its cycle time to less than 10 minutes. Further shortening is required in order to be applied to the mass production of cars since the production cycle time needs to be less than 1 minute. Therefore the thermoforming process of carbon fiber reinforced thermoplastic (CFRTP) has increased its presence in the industry since it is a faster manufacturing process than RTM process which needs a long curing stage.

Finite element analysis (FEA) as an alternative approach for experimental study is effective in designing fiber reinforced plastic products because there are many design parameters such as fiber type, resin type, morphology of fiber, volume fraction of fiber, fiber orientation, etc. Forming simulation is especially important because the performance of the final composite part strongly depends on changes in fiber orientation during the forming process. Prediction of wrinkle as well as fiber orientation is important because wrinkles are one of the major forming defects that dramatically decrease the compressive strength. The simulation models in many of existing researches [1-3] ignore bending stiffness as it is significantly low compared to tensile stiffness; notwithstanding bending stiffness plays a very important role in the prediction of wrinkles.

This study proposes a model for FEA that can consider the out-of-plane bending stiffness as well as the in-plane anisotropic properties of textile reinforcement. Furthermore the textile reinforcement FE model is extended to the thermoplastic pre-preg for thermoforming simulation. At first, hemispherical forming simulations of textile reinforcement are conducted in order to verify the influence of the out-of-plane bending stiffness upon the wrinkles by comparing with those of a meso-scale model as reference. The results using this proposed model are in good agreement with the meso-scale model results. As the next step, a model of thermoplastic pre-preg which can consider the temperature dependent in-plane and out-of-plane properties is constructed based on the results of bias-extension and three-point bending experiments which are conducted in the range of the process temperatures. S-rail thermoforming simulations are performed and compared to experimental results. Simulated outline and shear angle are in good agreement with experimental results. Moreover, sensitivity study analysis suggests that the effect of the temperature plays a dominant role in deformation during thermoforming processes.

## 3 Preform simulations of dry textile reinforcement for RTM process

RTM usually involves textile reinforcement and consists of three process stages. First, form the textile reinforcement. Second, inject resin into this preformed textile reinforcement and then, cure it to create

the final composite part as the final stage. The forming simulation of the dry textile reinforcement at the first stage in RTM is discussed in this chapter.

### 3.1 Specific mechanical behavior of textile reinforcement

In our previous study [4], we performed simulations using the meso-scale model under tensile, shear and bending deformations in order to understand each behavior. The tensile stiffness in yarn direction is much higher than the shear and bending as shown in Fig.1. Furthermore, bending stiffness differs depending on the direction of the yarn.

The bending behavior of textile reinforcement is complex due to the intricate interactions of the yarns and fibers. Although the bending stiffness is often ignored as it is very low compared to tensile stiffness, more accurate simulation is achievable by considering bending stiffness in forming simulation. This improvement of the accuracy is especially remarkable for wrinkling as mentioned above.

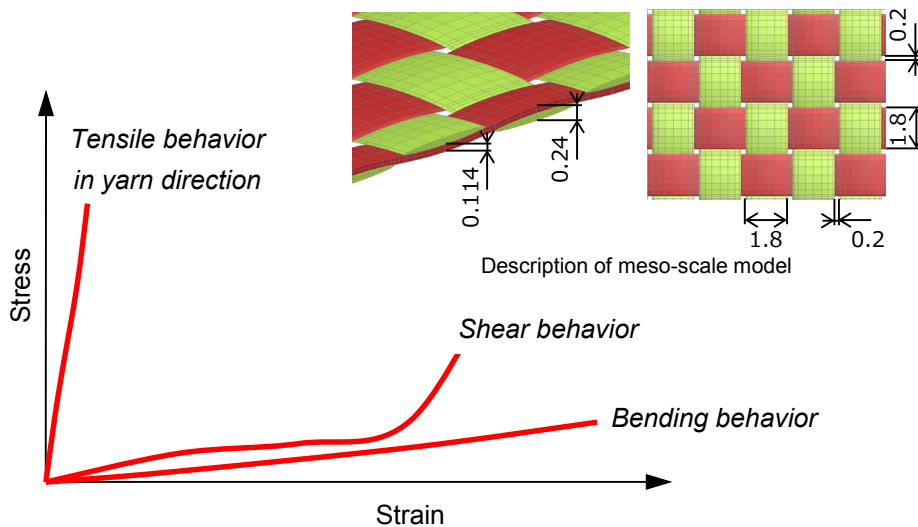


Fig.1: Mechanical behavior of textile reinforcement simulated by meso-scale model.

### 3.2 Shell and membrane hybrid model

Shell elements are usually used in sheet metal forming simulation. The out-of-plane bending stiffness of a continuous material such as metal can be directly deduced from in-plane properties. However, the textile reinforcement simulation using shell elements shows that the derived bending stiffness is unrealistically high compared to the experimental bending stiffness. In order to describe the very low out-of-plane bending stiffness at macroscopic scale, it is possible to use the extremely small transverse shear stiffness in a Reissner-Mindlin shell where the transverse shear deformation is capable. However it is very difficult to measure the transverse shear property of textile reinforcement by experimental approach.

Thus we propose the shell and membrane hybrid model in order to consider the bending stiffness that is independently free from any in-plane properties. Fig.2 shows the composition of our proposed model.

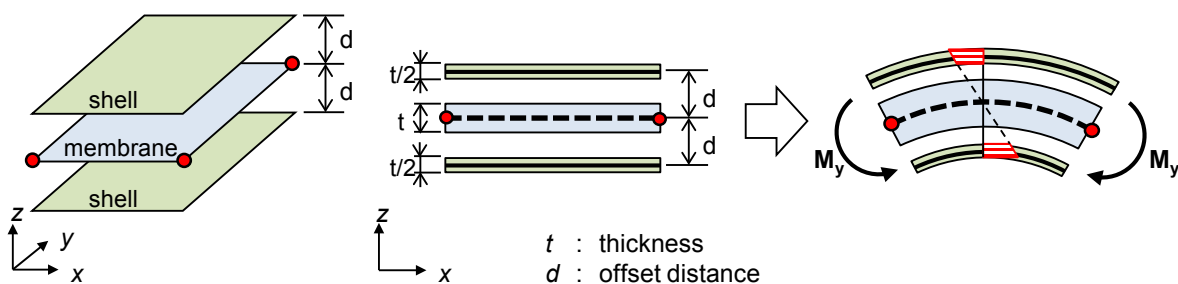


Fig.2: Shell and membrane hybrid model considering in-plane and out-of-plane properties.

In-plane properties are described by the membrane element and the bending stiffness is represented by a set of elements which consist of two shell elements with the membrane element in between. Shell elements are placed on either side of the membrane element to couple bending stiffness to it. The offset of the shell reference surface is applied to increase the effect of bending stiffness. As a result, we can give a small Young's modulus to the two shell elements. It is enough to get effective bending stiffness, but not enough to affect the in-plane properties. It is assumed that there is no interaction between the bending stiffness and in-plane deformation.

### 3.3 Influence of out-of-plane bending stiffness on wrinkling during forming

A blank-holder is often used to reduce wrinkles. But as a first step, hemispherical forming simulations are conducted without a blank-holder in order to verify the influence of the out-of-plane bending stiffness upon wrinkling under a severe condition, using both the meso-scale and the proposed model. The size of the blank sheet of textile reinforcement is 156 mm x 156 mm. The radius of the hemispherical part of the punch is 50 mm and the travelling distance of the movable punch is 30 mm. In this study, **\*MAT\_VISCOELASTIC\_LOOSE\_FABRIC (234)** is adapted to the membrane element within our proposed shell and membrane combined model in order to describe the in-plane behavior. This model of woven textiles can account for the stress component due to the yarn rotational friction as well as the trellising with reorientation of the yarns and their locking. Moreover the effects of off-axis bending stiffness can be calculated by giving an orthotropic material formulation, **\*MAT\_ORTHOTROPIC\_ELASTIC (002)**, to the shell elements. The material properties defined in these models are derived from meso-scale simulations [4].

Fig.3 shows the FE model and the deformed shapes of the meso-scale model. The model which consists of only membrane elements is also calculated to investigate the effect of the bending stiffness. Many small wrinkles are observed in the model which considers only in-plane properties. The proposed model considers out-of-plane bending stiffness as well as in-plane properties. The shapes of wrinkles in the proposed model are similar to the ones in the meso-scale model. Here the simulations demonstrate that the bending stiffness plays a very important role in the shapes of wrinkles.

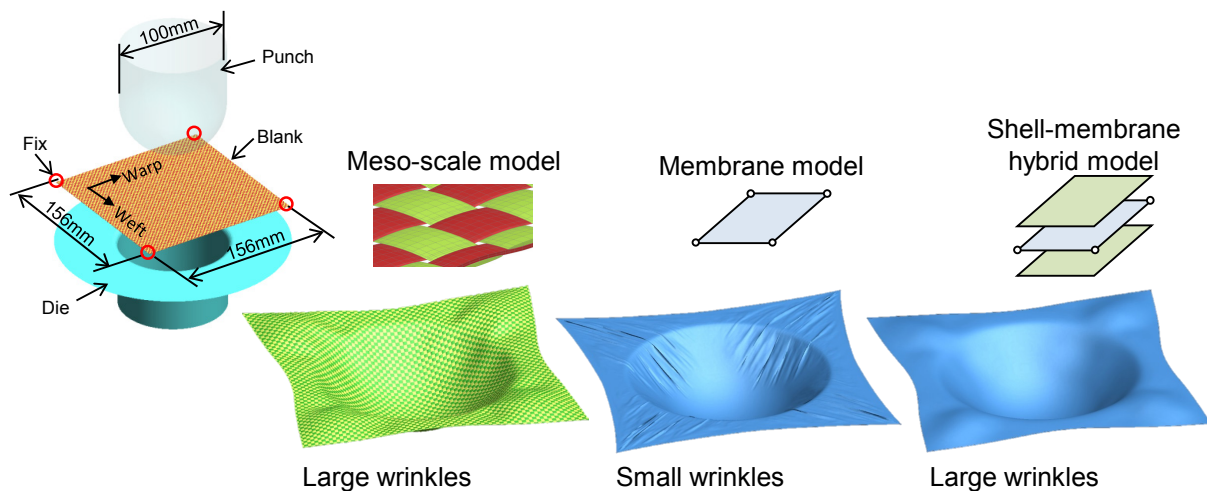


Fig.3: FE model without blank-holder and comparison of wrinkles.

## 4 Thermoforming simulation of thermoplastic pre-preg

The thermoplastic pre-pregs are stacked in the required orientation and are consolidated by a hot press. In the non-isothermal process, the pre-consolidated laminate is heated to forming temperature usually separately in an oven. The heated laminate is rapidly transferred to a forming tool. During forming the laminate is cooled by the contact with the tool. Pressure can be removed after the temperature of the laminate has been reduced to below the thermoplastic resin recrystallization level [5].

In this chapter, the development of the FE model of a textile thermoplastic pre-preg for non-isothermal forming is described. A forming simulation for non-isothermal process should be performed as a thermal-mechanical coupling analysis because the pre-preg temperature dramatically drops at and around the contact point with the tool and the material shows significant temperature dependent behavior.

#### 4.1 Thermoplastic pre-preg model

The objective is to extend the textile reinforcement model proposed in chapter 3 to the thermoplastic pre-preg model. In order to add the effect of thermoplastic resin to the textile reinforcement model, additional membrane elements are placed around the textile membrane. In-plane stress response of the pre-preg is represented in a parallel system of textile reinforcement and thermoplastic resin where those stresses are separately calculated. Fig. 4 shows the schematic of the thermoplastic pre-preg model for non-isothermal forming simulation.

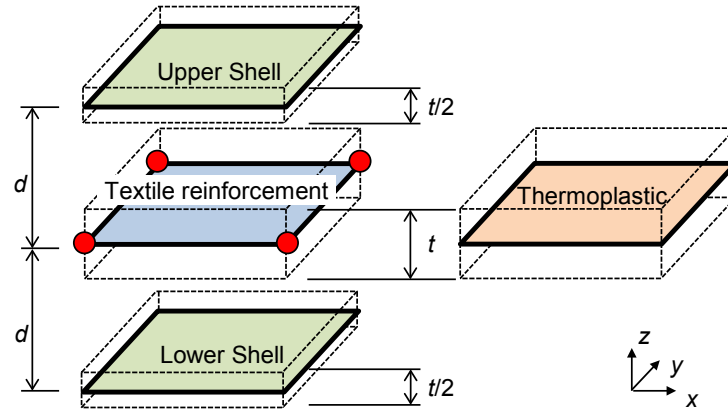


Fig. 4: Modeling schematic of textile thermoplastic pre-preg.

The thermoplastic material is `*MAT_ELASTIC_VISCOPLASTIC_THERMAL (106)` which considers thermal effects. The stress contribution of the thermoplastic in yarn direction, 0/90, is much less important than in 45/-45 direction since the stiffness of the yarn is much higher than the stiffness of the thermoplastic. Therefore the main purpose of the additive stress contribution of the thermoplastic on the textile is to describe the in-plane shear response of the pre-preg.

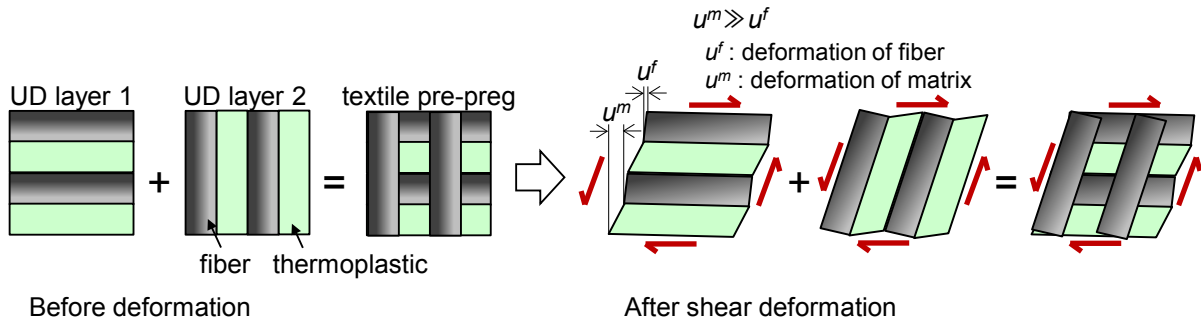


Fig. 5: Schematic illustration of textile as superposed two UD layers.

To simplify the meso-scale material structure, the textile pre-preg is made up of two different superposed layers which consist of unidirectional fibers (UD layer) as shown in Fig.5. The fiber direction of first layer is oriented initially at 90° with respect to the second layer. Each layer is deformed freely without any interaction. As a result of this simplified assumption, any effect of textile architecture becomes ignorable. Reuss model [6], which was developed from the assumption of equal stress in fiber and resin and is often used to predict the in-plane shear property of a UD material as an elementary micromechanical approach, can be adapted to the stress calculation of resin in each layer under in-plane shear deformation. The stress of the thermoplastic is calculated by:

$$\varepsilon_{ij}^m = \frac{\varepsilon_{ij} - V_f \varepsilon_{ij}^f}{(1 - V_f)} \quad (1)$$

Where  $\varepsilon_{ij}^m$  is a thermoplastic strain which is calculated based on Reuss model.  $\varepsilon_{ij}$  and  $\varepsilon_{ij}^f$  are the macro strain of the pre-preg and the fiber strain respectively.  $V_f$  is the fiber volume fraction. Here,  $\varepsilon_{ij} \gg \varepsilon_{ij}^f$  because the fiber stiffness is usually much higher than resin stiffness,  $\varepsilon_{ij}^m$  can be approximated as:

$$\varepsilon_{ij}^m = \frac{\varepsilon_{ij}}{(1 - V_f)} \quad (2)$$

Elements for the textile model and the thermoplastic model undergo the same displacement as they are represented in a parallel system. However the strain of the thermoplastic is calculated by introducing eq. (2).

## 4.2 Material characterization of thermoplastic pre-preg

The textile thermoplastic pre-preg tested in this work is composed of plain weave carbon fiber fabric and polymethyl-methacrylate (PMMA) resin. PMMA is a thermoplastic polymer. The temperature of glass-liquid transition ( $T_g$ ) of PMMA is 108°C. Pre-consolidated laminate that has four pre-preg layers is produced by a hot press at a temperature above the melting point of PMMA.  $V_f$  of the laminate after pre-consolidation is 70% and the thickness of the laminate with 4 ply is 0.84mm on average.

### 4.2.1 In-plane shear, bias-extension test

A large in-plane shear deformation typically occurs during the forming of a textile laminate since the in-plane shear resistance is very low until the textile laminate reaches the shear locking angle. Thus accurately expressing the in-plane shear behavior of a textile laminate is very important for accurate forming simulation as mentioned before. A bias-extension test is a popular approach to measure the shear property of a textile laminate. It is a tensile test performed on a rectangular specimen where the warp and weft yarns are oriented initially 45/-45 to the direction of applied tensile load. In this study, bias-extension tests were performed at five different temperatures, 50, 100, 150, 180 and 200°C.

Simulations of the bias-extension tests are also performed at five different temperatures. The stress-strain relationships of PMMA under  $T_g$ , 50 and 100°C, used for the simulations are taken from CAMPUS database [7]. Those over  $T_g$ , 150, 180 and 200°C are identified by fitting the experimental results since there is no database of stress-strain relationships over  $T_g$ . Fig. 6 shows comparisons of load responses between experimental measurements and simulations.

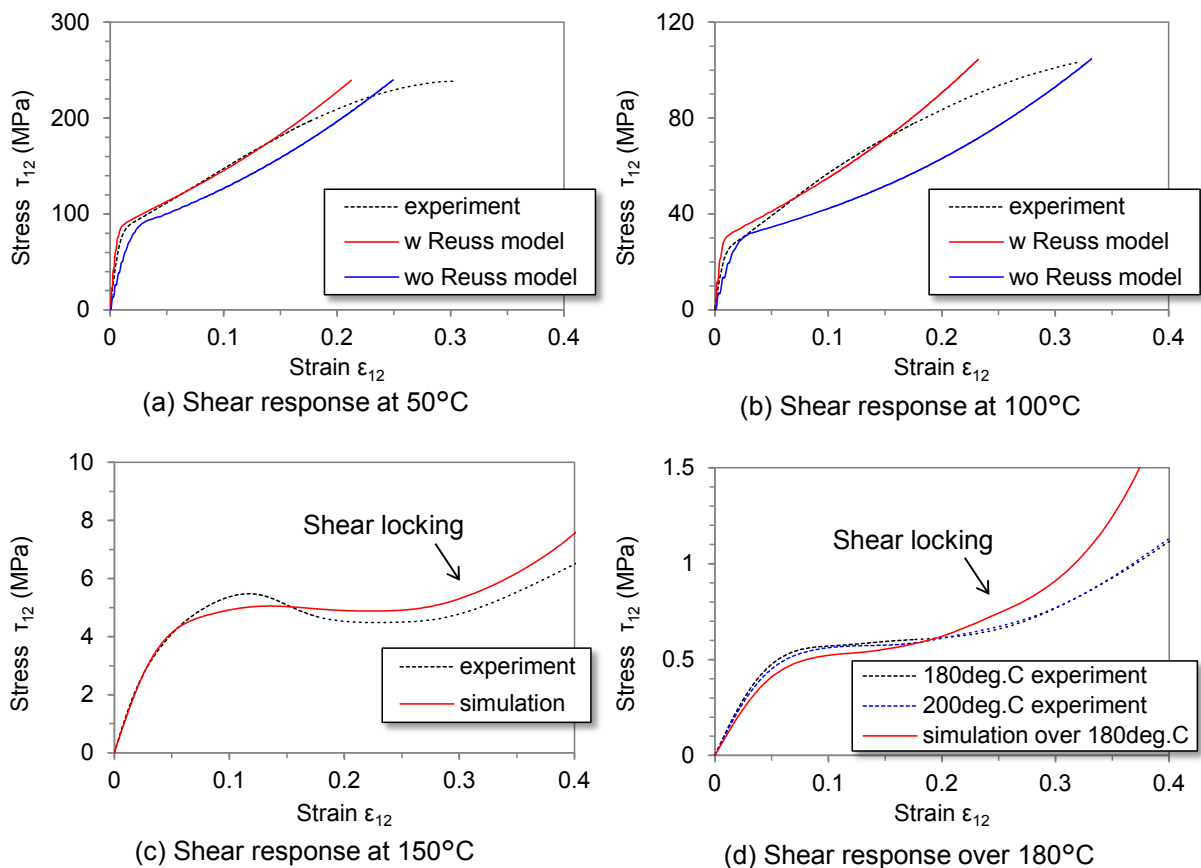


Fig.6: Comparisons of in-plane shear responses under bias-extension tests.

From the experimental measurements (black and blue dot lines in Fig.6), the temperature dependent shear property has to be considered, especially for non-isothermal forming because the in-plane shear property strongly depends on temperature during the forming. The experimental results at 180 and 200°C were similar to each other. At temperatures higher than  $T_g$ , we observed the peeling of the interlayer and squeeze flow of thermoplastic resin after the shear locking. At the same time, the jagged edge found after the bias-extension test revealed that the test had induced intra-ply slip between yarns as well as trellising after shear locking. Thus we understand the bias-extension test results appear to be valid before it reaches the shear locking angle.

The simulations of the bias-extension tests have been done by LS-DYNA with the proposed thermoplastic pre-preg model. The simulation responses are shown in Fig. 6 (red solid lines), along with the experimental measurements. Regarding the temperature range under  $T_g$ , Fig. 6 (a) and (b), red lines show the results of simulation applying Reuss model. On the other hand, blue lines show the results of simulation using original stress-strain relationship of PMMA not applying Reuss model. We can see the shear response applying Reuss model is more similar to that of experiments than the result not applying Reuss model. Regarding the temperature range over  $T_g$ , a good correlation with the experimental force up to shear locking angle over  $T_g$  is obtained by adjusting the properties of PMMA.

#### 4.2.2 Out-of-plane bending, 3-point bending test

Next, we conducted 3-point bending tests at three different temperatures, 50, 75 and 100°C in order to understand the temperature dependent bending property. The simulations of 3-point bending tests were also conducted using `*MAT_ELASTIC_VISCOPLASTIC_THERMAL (106)` to the upper and lower shell elements in order to describe the temperature dependent out-of-plane bending behavior. Fig. 7 shows the comparison between the experimental results and simulated results. We can see good agreements up to a maximum flexural stress at every temperature.

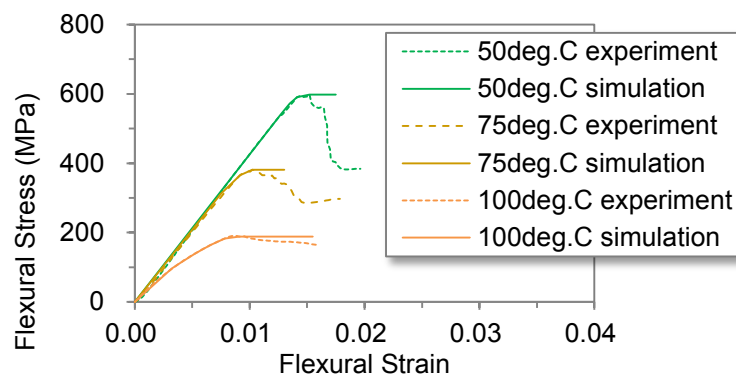


Fig.7: Comparison of out-of-plane bending responses under 3-point bending tests.

#### 4.3 S-rail thermoforming simulations and sensitivity study

Pre-consolidated laminates consist of four textile thermoplastic pre-preg layers. Simple laminates with  $[(0/90)]_4$  and  $[(45/-45)]_4$  lay-ups were tested experimentally in order to assess the capability of the proposed FE model. S-rail forming experiments were performed with a non-heated metal tool at room temperature. First, the pre-consolidated laminate was heated to forming temperature separately in an oven. Then it was rapidly transferred to a forming tool and formed by the downward movement of the punch at a speed of 20mm/s. The temperature of the laminate, which was measured just before the forming process, was uniformly distributed over the majority of the surface area. Its average temperature was 185°C which were measured by thermography.

Simulations are also performed by two different approaches to investigate the effect of the change in the temperature during the forming. One is non-isothermal simulation by thermal-mechanical coupling analysis which can consider the change in the temperature during forming. The other is isothermal simulation by simple mechanical analysis under the assumption of a constant temperature during the forming process. In non-isothermal forming simulation, the heat transfer conductance between pre-preg laminate and tool is determined by reference to the database of the commercial plastics injection molding software Mox3D [8]. Thermal conductivity of the pre-preg laminate is calculated by Eshelby-based semi-analytical mean-field homogenization approaches in Digimat-MF [9]. Fig. 8 shows the simulation model. Slippage between the neighboring layers is not taken into account in this study because there was no slippage observed in the experiments.

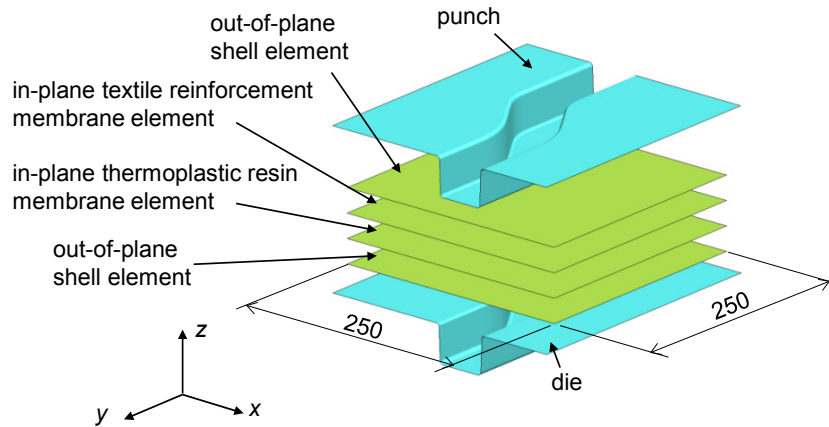


Fig. 8: S-rail thermoforming simulation model of pre-consolidated laminate.

Fig. 9 shows the comparisons of the outlines between the experiments and each simulation. The outlines simulated by the non-isothermal simulations show good agreement with the experimental measurements for both laminates with  $[(0/90)]_4$  and  $[(45/-45)]_4$  lay-ups. On the other hand, the outlines simulated by the isothermal simulations are different from the experimental measurements for both lay-ups.

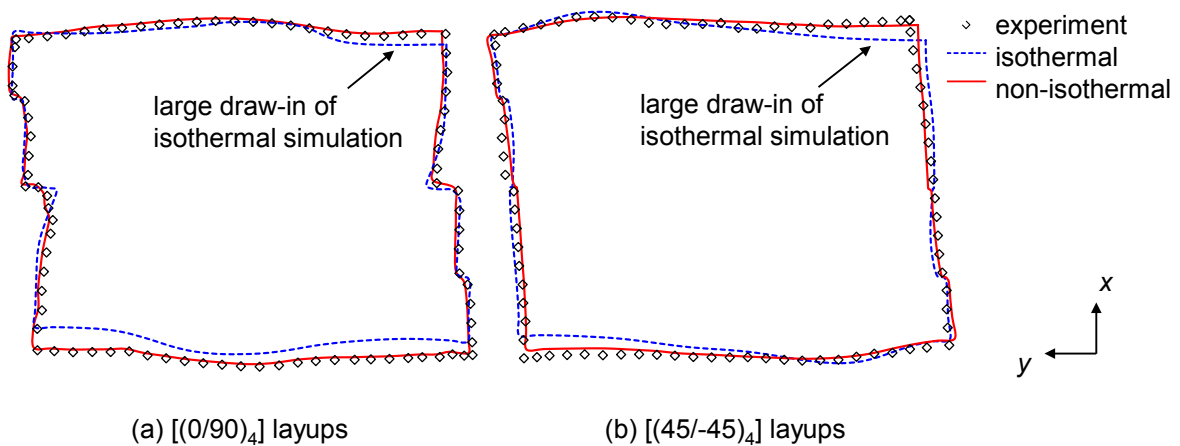


Fig. 9: Comparison of final outlines between experiments and simulations.

Fig. 10 shows the distributions of the temperature in the laminate of the  $[(0/90)]_4$  lay-up in the non-isothermal simulation. It describes that the temperature of the laminate in the side wall near the corner of punch drops during the forming process. This drop is due to contact with the tools from both sides. The shear resistance is dramatically increased by the decreased temperature.

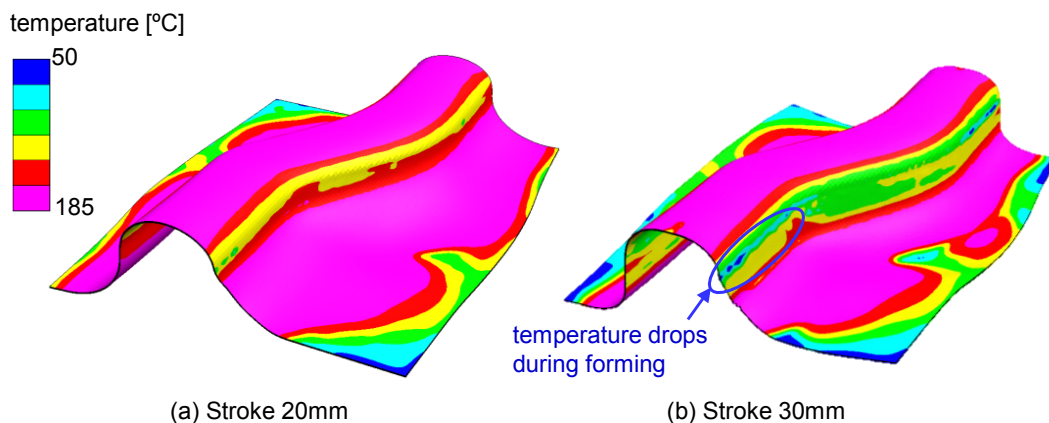


Fig. 10: Temperature distribution during non-isothermal forming simulation of  $[(0/90)]_4$  layups.

Consequently, the shear deformation in the isothermal simulation is larger than the experiment and the non-isothermal simulation: 71° for the experiment, 61° for the isothermal simulation and 71° for the non-isothermal simulation as shown in Fig. 11. This is the reason for the larger draw-in in the isothermal simulation. These simulation results demonstrated that formability is significantly changing throughout the non-isothermal forming.

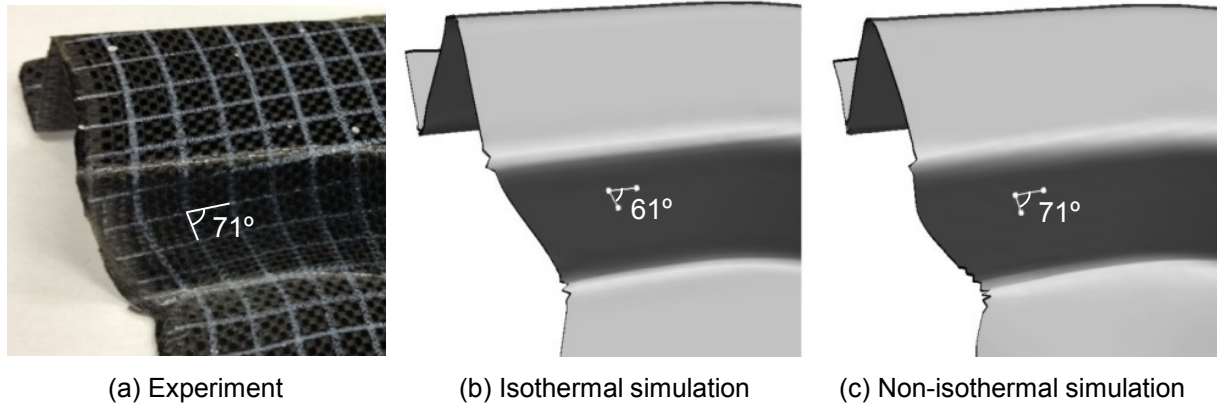


Fig.11: Comparison of shear angle between experiment and simulations of [(0/90)<sub>4</sub>] layups.

## 5 Summary and outlook

An FE model for the forming of textile reinforcement was proposed in this study. The proposed model overcame the bending stiffness by placing shell elements on both sides of a membrane element. To verify the model, hemispherical forming simulations were conducted for a purpose of comparison of the model with the meso-scale model. The proposed model showed to be in good agreement with the meso-scale model. The results of sensitivity studies showed that an accurately described bending stiffness was very important for evaluating wrinkles.

Furthermore, we extended the textile reinforcement model to a thermoplastic pre-preg model for non-isothermal forming simulation. This model has the capability to consider the change in temperature during forming and the temperature dependent material property by thermal-mechanical coupling analysis. For the effect of the temperature dependent material behavior on the forming simulation results, S-rail forming simulations of pre-preg laminate were conducted as well. Results of this sensitivity study pointed out that considering the effect of the temperature is important to accurately predict deformation during non-isothermal forming. The deformations predicted by the proposed model agreed well with experimental results.

Now, JSOL Corporation is developing a software tool for the forming simulation of dry textile reinforcement, textile pre-preg and UD pre-preg. The following features are planned:

- Material database tool
  - ✧ Manage the material database
  - ✧ Automatic creation of material model based on the experimental results
  - ✧ Define material properties for in-plane and out-of-plane properties independently
  - ✧ Consider the temperature dependent material properties of thermoset and thermoplastic pre-pregs
- Layup definition tool
  - ✧ Define number of plies, orientation and thickness
  - ✧ Automatic creation of multi-layer model for LS-DYNA. The individual layers consist of membrane and shells.
  - ✧ Automatic definition of contact between plies  
(Coulomb friction models as function of the Hersey number [10-11] were implemented as a user friction model.)

This software tool enables users to optimize process condition, and minimize lead times and design costs.



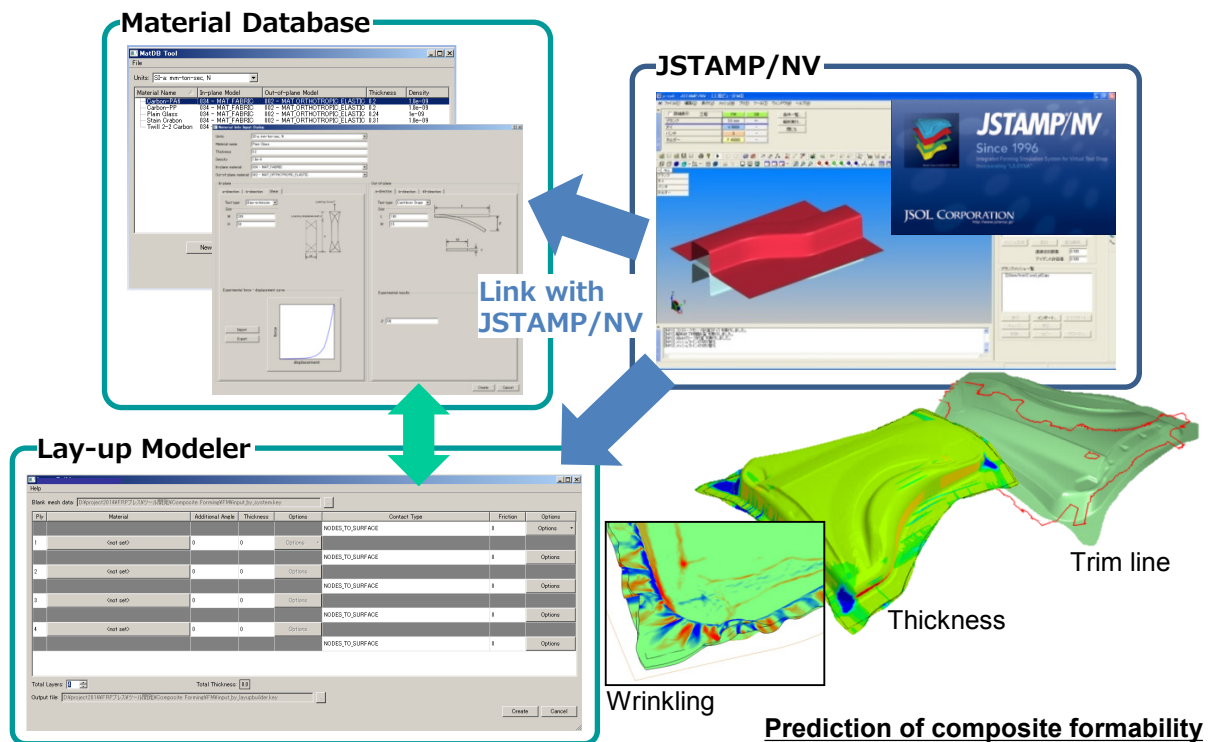


Fig.12: Software tools for composite forming simulation linking with JSTAMP/NV.

## 6 Acknowledgments

The experiments of thermoforming of thermoplastic pre-pregs were conducted at Asano Corporation. The work was funded by Strategic Foundational Technology Improvement Support Operation 2012-2014. The good support is gratefully acknowledged.

## 7 Literature

- [1] A. Willems, S. V. Lomov, I. Verpoest, D. Vandepitte, P. Harrison, W. R. Yu, "Forming simulation of a thermoplastic commingled woven textile on a double dome", International Journal of Material Forming, vol.1, 2008, pp.965-968.
- [2] R.H.W. ten Thije, R. Akkerman, "A multi-layer triangular membrane finite element for the forming simulation of laminated composites", Composites Part A: Applied Science and Manufacturing, vol.40, 2009, pp.739-753.
- [3] Y. Aimene, E. Vidal-Sallé, B. Hagege, F. Sidoroff, P. Boisse, "A hyperelastic approach for composite reinforcement large deformation analysis", Journal of Composite Materials, vol.44, 2010, pp.5-26.
- [4] M. Nishi, T. Hirashima, "Approach for dry textile composite forming simulation", Proceedings of 19th International Conference on Composite materials (ICCM-19), 2013, pp.7486-7493
- [5] A.C. Long, "Composite forming technologies", CRC Press, Woodhead Pub.: Cambridge, UK, 2007, pp.256-276.
- [6] D. Hull, T.W. Clyne, "An Introduction to Composite Materials", Cambridge University Press, 1996, pp.60-77.
- [7] CAMPUS, Available: <http://www.campusplastics.com/campus>
- [8] Molex3D, Available: <http://www.moldex3d.com/en/>
- [9] Digimat-MF, Available: <http://e-xstream.com/product/digimat-mf>
- [10] P. Wang, N. Hamila, P. Boisse, "Thermoforming simulation of multilayer composites with continuous fibres and thermoplastic matrix", Composites Part B: Engineering, vol.52, 2013, pp.127-136.
- [11] S.P. Haanappel, R.H.W. ten Thije, U. Sachsa, B. Rietman, R. Akkerman, "Formability analyses of uni-directional and textile reinforced thermoplastics", Composites Part A: Applied Science and Manufacturing, 2014, vol.56, pp.80-92.